



1 Exploring the role of hydrological pathways in modulating North Atlantic Oscillation (NAO)  
2 teleconnection periodicities from UK rainfall to streamflow.

3 William Rust<sup>a</sup>; Mark Cuthbert<sup>b</sup>; John Bloomfield<sup>c</sup>; Ron Corstanje<sup>d</sup>; Nicholas Howden<sup>e</sup>; Ian Holman<sup>a</sup>

4 <sup>a</sup> Cranfield Water Science Institute (CWSI), Cranfield University, Bedford MK43 0AL

5 <sup>b</sup> School of Earth and Ocean Sciences, Cardiff University, Park Place, Cardiff, CF10 3AT

6 <sup>c</sup> British Geological Survey, Wallingford, OX10 8ED

7 <sup>d</sup> Centre for Environment and Agricultural Informatics, Cranfield University, Bedford MK43 0AL

8 <sup>e</sup> Queen's Building, University Walk, Clifton BS8 1TR

9

10 Correspondence to William Rust (w.d.rust@cranfield.ac.uk)

11 Abstract

12 An understanding of multi-annual behaviour in streamflow allows for better estimation of the  
13 risks associated with hydrological extremes. This is can enable improved preparedness for  
14 streamflow-dependant services such as freshwater ecology, drinking water supply and  
15 agriculture. Recently, efforts have focused on detecting relationships between long-term  
16 hydrological behaviour and oscillatory climate systems (such as the NAO). For instance, the  
17 approximate 7-year periodicity of the NAO has been detected in groundwater level records in  
18 the North Atlantic region, providing a degree of forecasting for future water resource extremes  
19 due to their repeating, periodic nature. However, the extent to which these 7-year NAO-like  
20 signals are propagated to streamflow, and the catchment processes that modulate this  
21 propagation, are currently unknown. Here, we show statistically significant evidence that these  
22 7-year periodicities are present in streamflow (and associated catchment rainfall), by applying  
23 multi-resolution analysis to a large dataset of streamflow and associated catchment rainfall  
24 across the UK. Our results provide new evidence for spatial patterns of NAO periodicities in  
25 UK rainfall with areas of greatest NAO signal found in south west England, South Wales,  
26 Northern Ireland and central Scotland, and that NAO-like periodicities account for a greater  
27 proportion of streamflow variability in these areas. Furthermore, we show that subsurface  
28 pathway contribution, as characterised by the Baseflow Index (BFI), and the response times  
29 of subsurface pathways, as characterised by Groundwater response Time (GRT), are  
30 influential factors for streamflow sensitivity to these NAO-like cycles. Our results provide



31 critical process understanding for the screening and use of streamflow teleconnections for the  
32 improving the practice and policy of long-term streamflow resource management.

33

#### 34 1. Introduction

35 The North Atlantic Oscillation (NAO) is a dipolar system of atmospheric pressure in the North  
36 Atlantic region that is known to modulate European meteorological and hydrological conditions  
37 (Hurrell and Deser, 2010; Lawler et al., 2011; Faust et al., 2016; West et al., 2019). It has been  
38 shown that the winter state of the NAO drives wetter or drier conditions in rainfall and river  
39 flow in the same winter season (Uvo, 2003; Bouwer et al., 2006; Fritier et al., 2012; Riaz et  
40 al., 2017), by modulating the westerly storm track (Trigo et al., 2002; Dawson et al., 2004) and  
41 Gulf Stream strength (Frankignoul et al., 2001; Chaudhuri et al., 2011; Watelet et al., 2017).  
42 As such, this teleconnection has been shown to account for the majority of European winter  
43 water balance variability, and is particularly influential in western Europe (Alexander et al.,  
44 2005; López-Moreno et al., 2011).

45

46 In addition to sub-annual variability, the NAO exhibits a principal multi-annual cycle of between  
47 6 and 9 years (Hurrell, 1995; Hurrell et al., 2003; Zhang et al., 2011). Much research has  
48 focused on detecting the propagation of these multi-annual signals to hydrological records,  
49 given their potential to improve long-term projections of hydrological extremes (Tabari et al.,  
50 2014; Su et al., 2017; Rust et al., 2019). To date, NAO-like multi-annual cycles have been  
51 detected principally in groundwater level records in the USA (e.g Kuss and Gurdak, 2014),  
52 continental Europe (e.g. Neves et al., 2019) and the UK (e.g. Holman et al., 2011; Rust et al.,  
53 2019), in part due to the relative sensitivity of groundwater stores to long-term changes in  
54 recharge (Bloomfield and Marchant, 2013; Frootan et al., 2018; Van Loon, 2015).  
55 Furthermore, Rust et al (2019) compared NAO-like periodicities in composite rainfall records  
56 and groundwater levels in the UK's principal aquifers, demonstrating the degree to which



57 periodic NAO teleconnection signals can be modulated through part of the hydrological cycle.  
58 Given the presence of these multi-annual cycles in both UK rainfall and groundwater records,  
59 it follows that these signals may be propagated to streamflow, particularly in groundwater-  
60 dominated streams such as those found in many parts of southern and eastern England  
61 (Bloomfield et al., 2009). High baseflow streams are often critical for the function of public  
62 water supply, freshwater ecosystems, and provide a greater amenity value for surrounding  
63 areas (Acreman and Dunbar, 2004). Therefore, an understanding of the catchment processes  
64 that modulate teleconnection-driven multi-annual extremes in streamflow may provide a new  
65 opportunity to better manage the long-term use and sustainability of these streamflow-  
66 dependant services (Acreman and Dunbar, 2004; Chun et al., 2009). While existing studies  
67 have shown that the winter-averaged NAO can modulate streamflow in the UK at an annual  
68 scale (Kingston et al., 2006), the strength and spatiality of NAO-like multi-annual cycles in  
69 streamflow, and the catchment processes that modulate them, have yet to be assessed.

70

71 Hydrological pathways are often used to conceptualise the propagation of effective rainfall  
72 signals (rainfall minus evapotranspiration) through a catchment to streamflow (Misumi et al.,  
73 2001; Bracken et al., 2013; Crossman et al., 2014; Lane et al., 2019). For example, surface  
74 pathways are the result of infiltration- or saturation-excess runoff from the land surface and  
75 provide a direct response to rainfall in the order of hours or days (Nathan and McMahon, 1990;  
76 Gericke and Smithers, 2014; Kronholm and Capel, 2016). Subsurface pathways (such as the  
77 travel of water through the unsaturated zone and groundwater flow paths to channel baseflow)  
78 exhibit generally lower celerities than surface pathways and can produce a protracted  
79 response to rainfall in the order of months or years where faster subsurface pathways  
80 dominate (Carr and Simpson, 2018; Hellwig and Stahl, 2018), but ranging to decades or even  
81 millennia for longer, deeper groundwater flow pathways with low hydraulic diffusivity  
82 (Rousseau-Gueutin *et al.*, 2013; Cuthbert *et al.*, 2019). Existing research into periodic NAO  
83 teleconnections with groundwater resources has highlighted the importance of subsurface



84 pathway responsiveness in modulating NAO-like signals in groundwater stores (Kuss and  
85 Gurdak, 2014; Neves *et al.*, 2019; Rust *et al.*, 2019). Where a groundwater resource receives  
86 a periodic recharge signal (such as those from a climatic teleconnection), Townley (1995)  
87 suggests that pathways with response times shorter than the period length will propagate  
88 these signals to baseflow more effectively, with minimal damping. Conversely, groundwater  
89 pathways with response times longer than the period length cannot convey these signals to  
90 the stream at a sufficient rate, meaning the amplitude of the periodic signal is damped as it  
91 passes through the aquifer. Therefore, in the case of streamflow, we may expect that;

- 92 i. the propagation of NAO-like multi-annual periodic signals from rainfall to  
93 streamflow is dependent on the relative contribution of surface and subsurface  
94 (e.g. groundwater) hydrological pathways within a catchment.
- 95 ii. response times of subsurface pathways will modulate the amplitude of multi-annual  
96 periodic signals in streamflow where they are propagated by subsurface pathways

97 Finally, these effects (modulation of NAO signal propagation by hydrological pathways) may  
98 be expected to differ between winter and summer streamflow. Catchments in the UK have  
99 been shown to receive the strongest NAO signals in winter rainfall (Alexander *et al.*, 2005;  
100 Hurrell and Deser, 2010; West *et al.*, 2019). However, given the degree of fine-scale variability  
101 seen in precipitation records (Meinke *et al.*, 2005), winter streamflow may contain a relatively  
102 low signal-to-noise ratio as surface (and some subsurface) hydrological pathways respond to  
103 rainfall within the same winter season. Conversely, slower subsurface pathways provide a  
104 protracted response to winter rainfall signals, and are generally accepted to filter finer-scale  
105 variability (Bloomfield and Marchant, 2013). As such, we may expect the NAO teleconnection  
106 to have a greater influence on summer streamflow in permeable catchments which have a  
107 greater contribution from sub surface pathways (baseflow), and proportionally less  
108 contribution from surface pathways. In these instances, we may expect the teleconnection  
109 between NAO and UK streamflow may be asymmetric between summer and winter. If multi-  
110 annual periodic signals in streamflow are present via a teleconnection with the NAO, their use



111 for improving long-term projection of hydrological extremes will rely on an understanding of  
112 the catchment processes that modulate the strength of these signals, and their seasonal  
113 sensitivities.

114

115 The aim of this paper is to assess the extent to which NAO-like multi-annual signals are  
116 propagated from rainfall to streamflow across the UK, and to assess how this is modulated by  
117 the relative contribution of faster and slower hydrological pathways.

118

119 This aim will be met by addressing the following research objectives:

- 120 1. Characterise the strength, statistical significance and spatial distribution of NAO-like  
121 multi-annual periodicities in rainfall and associated UK streamflow
- 122 2. Quantify the relationship between catchment pathway contribution and response times  
123 and the NAO teleconnection by comparing NAO-like periodicity strength in summer  
124 and winter streamflow.

125

126

127

## 128 2. Data and Methods

### 129 2.1. Streamflow data

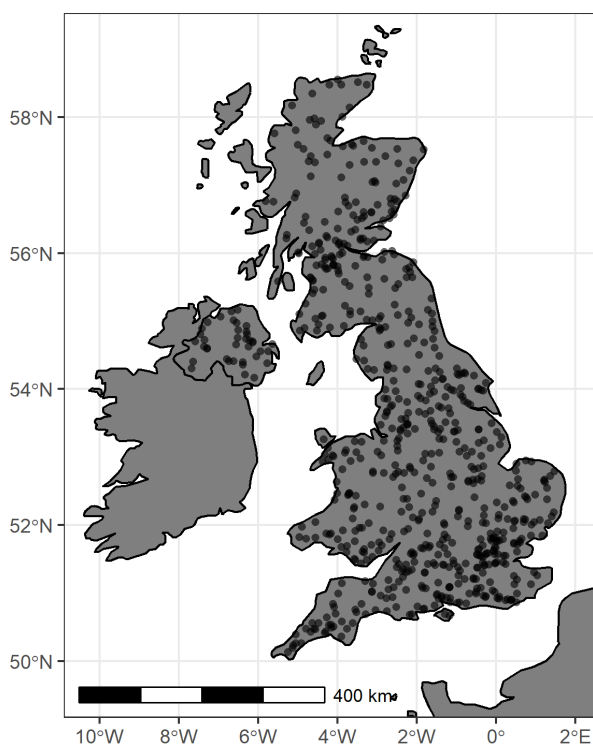
130 Monthly streamflow data and catchment metadata from the UK National River Flow Archive  
131 (NRFA; Dixon et al., 2013: <http://nrfa.ceh.ac.uk/>) has been used in this study. Gauging stations  
132 with more than 20 years of continuous streamflow data (and coincident catchment rainfall,  
133 discussed in the following section), and no data gaps greater than 12 months were initially  
134 selected. Where there were multiple gauging stations in a single named river catchment, only  
135 the sites with the largest catchment area were taken forward. This produced a final list of 705



136 streamflow gauging stations for use in this study. These streamflow records range from 20 to  
137 128 years in length, with a median length of 44.6 years (536 months). These sites provide a  
138 representative sample of sites from across the UK, with minimal bias towards the south of  
139 England, as indicated by Fig 1.

#### 140 2.1. Catchment Rainfall data

141 Calculated monthly rainfall totals for each streamflow gauge catchment are also provided by  
142 the NRFA. This dataset has been derived from CEH-GEAR data (Tanguy et al., 2016), which  
143 covers the 1890 – 2015 time period, using NRFA catchment boundaries. This catchment  
144 rainfall dataset has been used in multiple studies investigating catchment hydrology dynamics  
145 and catchment response to rainfall signals (Chiverton et al., 2015; Guillod et al., 2018; Gnann  
146 et al., 2019).



147

148 Figure 1 – Locations of streamflow gauges used in this study.



149

150

151 2.2. Catchment Metadata

152 In order to categorise the relative influence of surface and subsurface hydrological pathways  
153 on streamflow, the Base Flow Index (BFI) from the NRFA has been used for each streamflow  
154 gauge (Gustard et al., 1992). The BFI is a calculated proportion of the flow hydrograph  
155 (ranging from 0 to 1) that is derived from slower subsurface pathways such as groundwater-  
156 driven baseflow, where 1 is entirely baseflow. While empirical, BFI has been shown to be  
157 effective in relating physical catchment pathway processes to streamflow behaviour  
158 (Bloomfield et al., 2009; Chiverton et al., 2015). Figure 2a shows the spatial distribution of BFI  
159 across the UK. Higher BFI values are generally found in catchments with greater groundwater  
160 influence, such as those in southern and eastern England which are dominated by the UK's  
161 Chalk aquifer (Marsh and Hannaford, 2008). Areas of moderate BFI can also be found where  
162 there are substantial superficial or glacial deposits such as western England, central Wales  
163 and eastern Scotland. In this study, BFI has been grouped into "Low" (0 - 0.25), "Medium"  
164 (0.25 - 0.5), "High" (0.5 - 0.75) and "Very High" (0.75 - 1).

165 In addition to the BFI, the global dataset of Groundwater Response Times (GRT), developed  
166 by Cuthbert et al (2019), has been used in this study to estimate the responsiveness of  
167 unconfined subsurface pathways. GRT [T] can be conceptualised as a measure of the time  
168 required for a groundwater store to return to an equilibrium after a perturbation in recharge,  
169 and is given by:

$$\text{GRT} = \frac{L^2 S}{\beta T} \quad (\text{Eq.1})$$

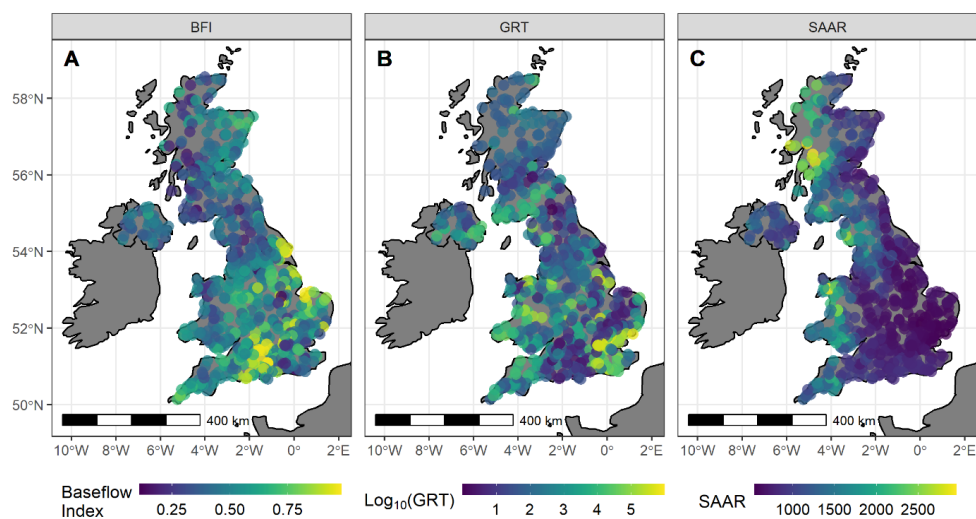
170 where  $\beta$  is a dimensionless constant,  $T$  is transmissivity [ $L^2 T^{-1}$ ],  $S$  is storativity [-] and  $L$  is the  
171 characteristic groundwater flow path length approximated for unconfined groundwater  
172 systems by the distance between perennial streams [L]. In this study, the mean GRT was  
173 taken for each of the NRFA catchments boundaries for each streamflow gauge.  $\text{Log}_{10}$  of GRT



174 is displayed in Fig. 2b for clarity purposes, as for gauge catchments used in this study the  
175 GRT ranges from approximately 1 year to approximately a million years (e.g. in very low  
176 permeability geological formations). While the mapping of GRT was carried out using global  
177 datasets with their inherent uncertainties, it should nevertheless enable categorisation of the  
178 likely timescales of groundwater response sufficiently well for the purposes of this paper. GRT  
179 is seen to be lowest (indicating shorter response times) in areas similar to areas of higher BFI;  
180 southern and eastern England. Lower GRT values are also seen in Northern England.  
181 Greatest GRT values are found in the south-east of England, and along the west coast of  
182 England and Wales. While BFI and GRT appear inversely similar in spatial extent, their  
183 correlation is low ( $r = -0.304$ ). This is to be expected as they measure different aspects of  
184 catchment process. Unlike BFI, which is an empirical measure of the degree to which slower  
185 pathways contribute to streamflow variability (which may encompass groundwater and  
186 throughflow), GRT is an estimate of the responsiveness of groundwater stores. In this study,  
187 GRT is grouped into five categories: 0-4 years 4-8 years; 8-16 years; 16-32 years and greater  
188 than 32 years.

189 Finally, Standard Average Annual Rainfall (SAAR) for the period 1961-1990 is also provided  
190 as metadata in the NFRA. While not used in our analysis, it is provided here to aid later  
191 discussion. There is a clear zonal divide in SAAR distribution in the UK with greater values on  
192 the west coast and lower values found on the east coast of the UK and central England.  
193 Greatest values are found in west Scotland.





194 Figure 2 – Spatial distribution of a. Base Flow Index (BFI), b.  $\text{Log}_{10}(\text{GRT})$  and c. Standard  
195 Average Annual Rainfall (SAAR) for each streamflow record.  
196

197

## 198 2.3. Methods

### 199 2.3.1. Data Pre-processing

200 In this study we follow a similar pre-processing methodology to that set out in Rust et al (2019).

201 The following pre-processing steps were undertaken. Firstly, all time-series were centred on  
202 the long-term mean and normalized to the standard deviation to produce a time series of  
203 anomalies. This is to allow spectra between rainfall and streamflow (and between sites across  
204 the UK) to be directly compared. From these anomalies; three time-series were created for  
205 both streamflow and rainfall, namely; monthly, winter-average (DJF) data and summer-  
206 average (JJA) data.

### 207 2.3.2. Continuous Wavelet Transform (CWT) and identification of Multi-annual periodic 208 signals

209 The CWT is a multi-resolution analysis use to quantify the amplitude of periodic components  
210 of a timeseries. It has been used increasingly on hydrological datasets to extract information  
211 on non-stationary periodic behaviours in rainfall (Rashid et al., 2015), river flow (Su et al.,



212 2017), and groundwater (Holman et al., 2011; Kuss and Gurdak, 2014). We use the package  
213 “WaveletComp” produced by Rosch and Schmidbauer (2018) for all transformations in this  
214 paper. The wavelet power,  $W$ , represents a dimensionless, absolute measure of periodic  
215 amplitude at a time index,  $t$ , and scale index,  $s$ , through a convolution of the data sequence  
216 ( $x_t$ ) with scaled and time-shifted versions of a wavelet:

$$W(\tau, s) = \frac{1}{s} \left| \sum_t x_t \frac{1}{\sqrt{s}} \psi * \left( \frac{t - \tau}{s} \right) \right|^2 \quad (\text{Eq. 2})$$

217 where the asterisk represents the complex conjugate,  $t$  is the localized time index,  $s$  is the  
218 wavelet scale, and  $dt$  is increment of time shifting of the wavelet. The choice of the set of  
219 scales,  $s$ , determines the wavelet coverage of the series in its frequency domain. The Morlet  
220 wavelet was favoured over other candidates due to its good definition in both the time and  
221 frequency domains (Tremblay et al., 2011; Holman et al., 2011). Since all datasets have been  
222 converted to anomalies prior to the CWT, the calculated wavelet power represents the relative  
223 strength of periodicities within the frequency spectra of the anomaly dataset. CWT was  
224 undertaken on all three dataset time resolutions (monthly, winter-average and summer-  
225 average) to gain an understanding of the periodicities within UK seasonal hydrological data.

226

### 227 2.3.3. Wavelet Significance Testing

228 Environmental datasets generally exhibit non-zero lag-1 autocorrelations (AR1) due to system  
229 storages (Meinke et al., 2005). As a result, they can produce low frequencies as a function of  
230 internal variance, rather than an external forcing (Allen and Smith, 1996; Meinke et al., 2005;  
231 Velasco et al., 2015). In order to assess whether the periodicities detected as part of the CWT  
232 are likely to be the result of noise within the dataset, a red-noise (AR1) significance test has  
233 been carried out on all wavelet transforms. For this, 1000 randomly constructed synthetic  
234 series with the same AR1 as the original time series were created using Monte Carlo methods.  
235 Wavelet spectra maxima from these represent periodicity strength that can arise from a purely



236 red noise process. Wavelet powers from the original dataset that are greater than these “red”  
237 periodicities are therefore considered to be driven by a process other than red noise, thus  
238 rejecting the null hypothesis. Teleconnection processes are often noisy meaning identification  
239 of significant periodic behaviours in hydrological datasets can be problematic (Rust *et al.*,  
240 2019). While we highlight any periodicities equal to or above a 95 % confidence interval (CI)  
241 ( $\leq 0.05$  p-values, due to convention), we also report the full range of p-value results in order  
242 to accrue an understanding of periodic forcing across the large dataset.

#### 243 2.3.4. Identification of likely NAO-driven periodicities in rainfall and streamflow

244 An exploratory approach was undertaken to identify the most prominent multi-annual  
245 periodicity across the streamflow records. Periods with a defined peak and greater than one  
246 year in length were identified within the monthly streamflow spectra. Records where no defined  
247 multi-annual peak in the wavelet power spectrum could be identified were ignored. The  
248 maximum wavelet power within the 25<sup>th</sup> and 75<sup>th</sup> percentile of the identified peak-periodicities  
249 was calculated for each of the streamflow and rainfall datasets, for all of the time resolutions.  
250 This produced a wavelet power for each dataset that is considered NAO-like, while minimising  
251 the influence of neighbouring periodicities. Since there is an expectation of spatially-varying  
252 NAO-like signal strength in rainfall (Rust *et al.*, 2018), it is necessary to minimise any  
253 confounding correlation between streamflow and rainfall NAO signals before testing  
254 streamflow NAO signals against catchment responsiveness. As such a residual NAO-like  
255 wavelet power was calculated for each of the streamflow spectra by subtracting the NAO-like  
256 wavelet power for the catchment rainfall from the streamflow wavelet power of the same site.  
257 This therefore also acts as a measure of the modulations of signal strengths between rainfall  
258 and streamflow. For the Summer streamflow NAO powers, a pragmatic decision was made to  
259 construct the residual using summer streamflow and winter rainfall, given the expected low  
260 signal presence in summer rainfall and the protracted influence of winter rainfall on summer  
261 baseflow. (Hannaford and Harvey, 2010). It is important to note that modulation, in this case,  
262 refers to a change in the spectral strength of NAO-like periods between rainfall and



263 streamflow, and not a measure of change in the amplitude of a temporally periodic behaviour  
264 between rainfall and streamflow.

265 2.3.5. Testing the relationship between NAO-like signal strength and hydrological  
266 pathway characteristics

267 In order to test the significance of the relationship between the BFI and GRT groups and NAO-  
268 like signal presence, the Mann Whitney U test (MWU) was undertaken. The MWU tests  
269 the null hypothesis that it is equally likely that a randomly selected value from one population  
270 will be different to a randomly selected value from a second population. We use this test here  
271 to investigate whether populations from each successive pair of ordinal groups (e.g. Low-Med  
272 for BFI) have significantly different distributions.

273 3. Results

274 3.1. Average wavelet power and p-values

275 Wavelet power spectra and p-values for each of the 705 streamflow and catchment rainfall  
276 records are displayed in Fig. 3 and 4 respectively. Average wavelet power and p-values across  
277 all sites are shown by the thick line in each plot. Wavelet power is a measure of the relative  
278 strength of periodic behaviour (periodicity) within a dataset. In the monthly streamflow and  
279 rainfall spectra figures, two discrete bands of periodicity can be seen in the average wavelet  
280 powers. These are centred on the 1-year and approximately 7-year periodicity; with average  
281 1-year wavelet powers of 0.661 (range: 0.113-0.980) for streamflow and 0.284 (range: 0.051-  
282 0.621) for catchment rainfall; and average 7-year wavelet powers of 0.056 (range: 0.002-  
283 0.360) for streamflow and 0.036 (range: 0.003 and 0.070) for rainfall. The ~7 year periodicity  
284 (P7) signal is also exhibited as discrete periodicities in the seasonal data; with mean P7  
285 wavelet powers of 0.274 (0.029 – 0.582) and 0.198 (0.010 – 0.571) for winter and summer  
286 streamflow; and 0.253 (0.015 – 0.472) and 0.107 (0.006 – 0.535) for winter and summer  
287 catchment rainfall respectively.



288 These strengths are generally reflected in the wavelet p-values, with bands of lower p-values  
289 at the 1 and ~7 year in monthly data, and ~7 year in the seasonal data. Wavelet p-values  
290 indicate the likelihood that the detected wavelet powers are not the result of external forcing.  
291 As such, lower values indicate increased significance of external forcing over the red noise  
292 null hypothesis. Wavelet p-values are generally lower in the monthly catchment rainfall spectra  
293 (0.002 – 0.996; mean of 0.289), compared with monthly streamflow (0 – 0.995; mean of 0.443),  
294 but this may be an artefact of longer autocorrelations in groundwater records relative to rainfall.  
295 Wavelet p-values are comparable for the seasonal spectra, with the exception of summer  
296 rainfall which shows the lowest significance; (winter rainfall; 0.003 – 0.995 (mean of 0.148);  
297 winter streamflow; 0.001 – 0.839 (mean of 0.129); summer rainfall; 0.005 – 0.992 (mean of  
298 0.462); summer streamflow; 0.000 – 0.997 (mean of 0.348)). Summer rainfall shows the  
299 weakest wavelet powers and greatest p-values for the P7 band.

300

301 Discrete bands of decreased average wavelet p-values can also be seen between 16-32 years  
302 for all the streamflow (monthly: 0.502, winter: 0.400, summer: 0.209) and rainfall datasets  
303 (monthly: 0.456, winter: 0.569, summer: 0.355). This periodicity band however exhibits  
304 negligible average wavelet power indicating minimal influence on variability. In the winter- and  
305 summer-average power spectra there is a band of increased strength at the 2-3 year  
306 periodicity. In the winter-average data there is no comparably low p-value, suggesting these  
307 higher powers are the result of noise within the averaged time series. However, all the summer  
308 spectra, appear to exhibit some decreased p-value at this 2-3-year band.

309

### 310 3.2. Spatial distribution of Wavelet Powers

311 The main multi-annual periodicity detected in the winter and summer river flow data (~7 years)  
312 was mapped for seasonal catchment rainfall and streamflow in Fig. 5. The winter spatial  
313 distributions show three distinct areas of increased wavelet power and significance, shared



314 between catchment rainfall and streamflow. The largest area is located in the south-west of  
315 England and south Wales, extending north into the Midlands and east into the south east of  
316 England in the streamflow data. For rainfall, this area encompasses 101 of the 221 catchments  
317 with significant (greater than 95% CI) P7 wavelet power, and 224 of the 262 significant sites  
318 in streamflow. The two other areas of increased wavelet significance in rainfall and streamflow  
319 cover Northern Ireland (20 significant sites for rainfall; 12 for streamflow) and central Scotland  
320 (30 significant sites for rainfall; 25 for streamflow). There are also stronger P7 wavelet powers  
321 along the west coast of the UK in both winter rainfall and streamflow, however most significant  
322 powers ( $> 95\%$  CI) are found in England and Wales. Additionally, the location of the greatest  
323 wavelet powers differs between winter rainfall and streamflow. Winter rainfall shows higher  
324 wavelet powers along the south-west peninsula of England, and south Wales, whereas the  
325 greatest winter streamflow wavelet powers are found in South and south-eastern England and  
326 appear to be co-located over the Chalk and other principal aquifers (Allen et al., 1997).

327 Little spatial structure exists in P7 wavelet power and significance for the summer-average  
328 rainfall data. Some increased density in significance is seen towards the south coast of  
329 England; however, this may be due to the increased density of sites in this region as seen in  
330 Fig. 1, especially given the negligible average P7 wavelet strength displayed in Fig. 3.  
331 Conversely, summer-average river flows show some clear spatial structure of wavelet power  
332 and significance, in the South of England, where 51 of the 70 sites with significant P7 powers  
333 are located. Again, these sites appear to be co-located over the Chalk aquifer (Allen et al.,  
334 1997).

335

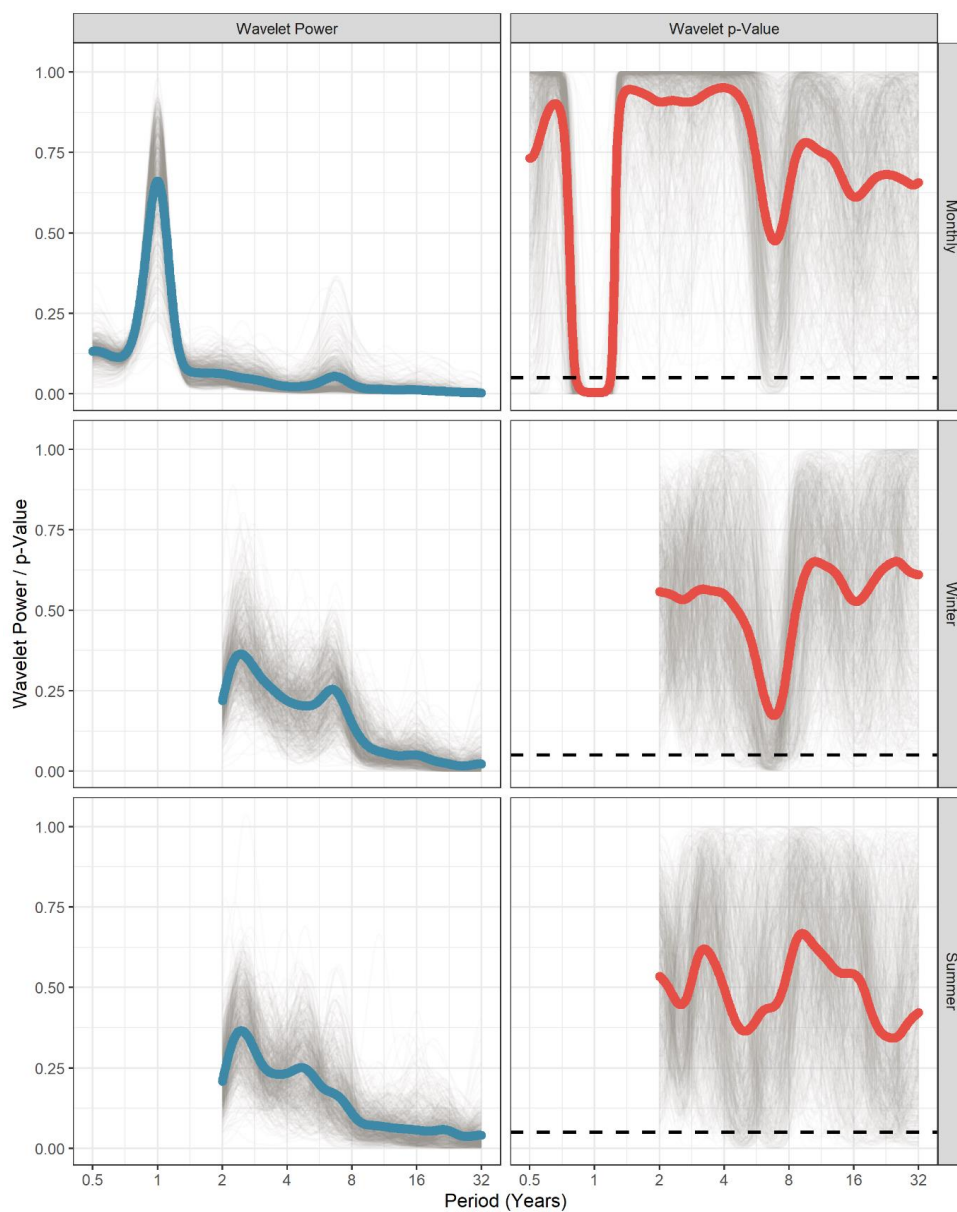
### 336 3.3. Testing of hydrological pathways

337 Figure 6 shows scatter plots of the P7 residual wavelet powers (RWP) for winter and summer  
338 streamflow plotted by BFI category (Fig. 6a), and a comparison of median P7 RWP with  
339 significance results from the MWU tests (Fig. 6b). Winter P7 median RWPs show a trend of



340 increasing wavelet powers with increasing BFI category, with the exception of between the  
341 Low and Medium categories (0.001, -0.002, 0.019 and 0.093 for Low, Medium, High and Very  
342 High groups respectively). A similar relationship is seen in the Summer median P7 RWP (-  
343 0.063, -0.079, -0.054 for Low, Medium and High groups), with a notably steeper increase for  
344 the final group when compared to winter P7 residuals (increasing to 0.101). This brings the  
345 median P7 residual powers for summer streamflow to a comparable magnitude to winter  
346 streamflow. In general, winter median P7 residual powers are close to zero except for the Very  
347 High category, indicating minimal modulation of P7 signal strength between rainfall and  
348 streamflow in the catchments with Low to High BFI. Summer P7 residuals are negative for  
349 Low – High BFI catchments indicating a reduction in P7 wavelet powers in streamflow  
350 compared to winter rainfall. The median P7 residual for sites in the Very High BFI is the only  
351 positive residual for summer streamflow, indicating an increase in relative P7 signal strength  
352 between winter rainfall and summer streamflow for these sites.

353 Figure 7 shows P7 RWP plotted against Groundwater Response Times (GRT) groups showing  
354 all gauges (Fig. 7a), and median RWP with significant results from the MWU tests (Fig. 7b).  
355 Winter streamflow shows higher, positive median RWP across all GRT groups (0.056, 0.079,  
356 0.017, 0.009, 0.002, for the 0-4, 4-8, 8-16, 16-32 and 32+ year groups respectively), whereas  
357 summer streamflow only shows positive RWPs for catchments in the 0-4 and 4-8 year GRT  
358 groups (median RWP of 0.014 and 0.024 respectively). GRTs groups greater than or equal to  
359 8 years all show negative median RWPs (-0.011, -0.058 and -0.074 for 8-16, 18-32 and 32+  
360 year groups respectively). Both winter and summer streamflow show decreasing median  
361 RWPs with increasing GRT, with the exception of the 4-8 year GRT group, which shows the  
362 greatest median RWP in both winter and summer. Significant difference between GRT groups  
363 are found between 0-4 and 4-8, and 4-8 and 8-16 for winter streamflow, and between 4-8 and  
364 8-16 for summer streamflow.

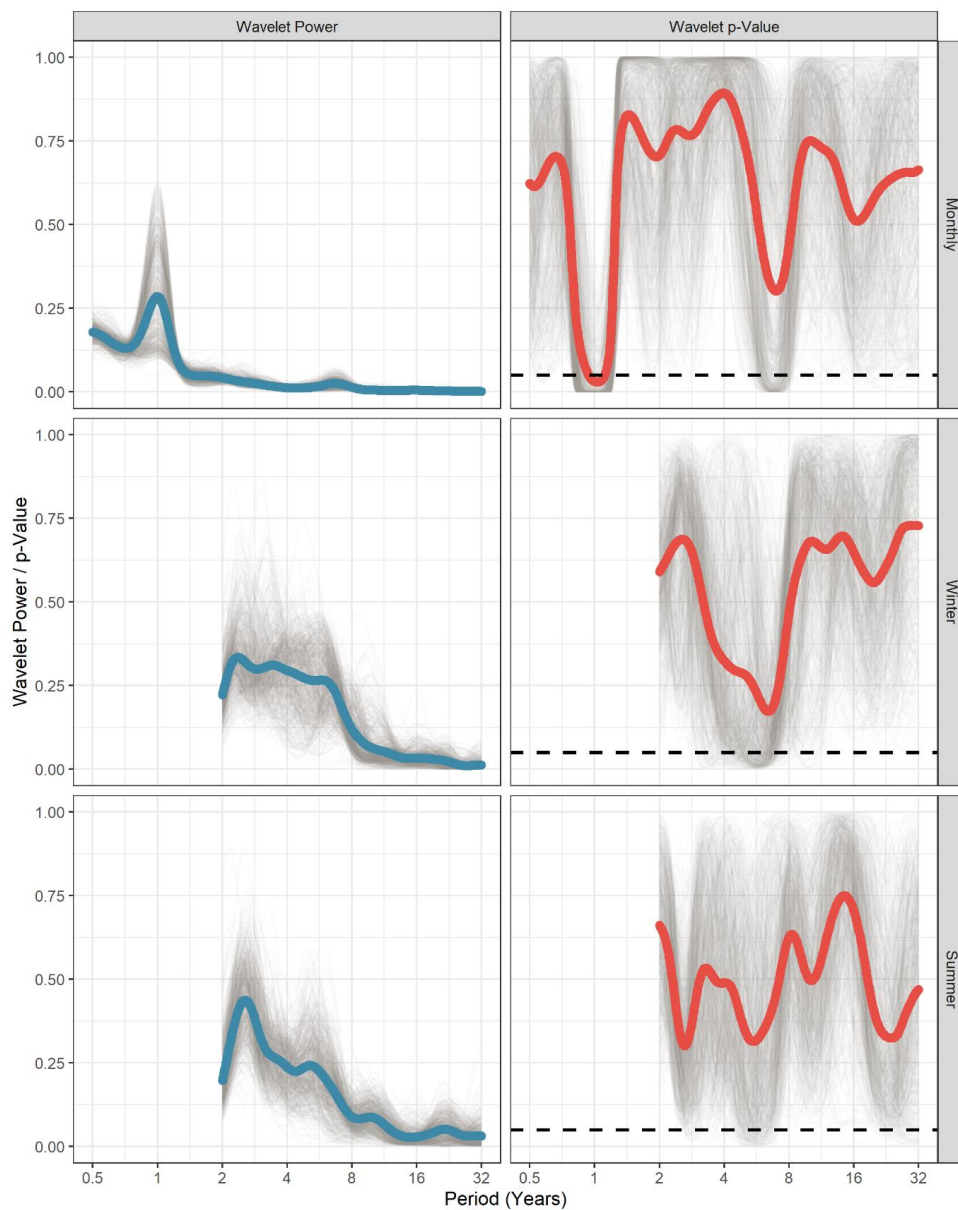


365

366 Figure 3 - Stacked streamflow wavelet spectra power (left) and p-values (right) from  
367 normalised Monthly, Winter and Summer resolution data of 705 catchments. 95% Confidence  
368 interval is shown as a dashed black line on the right column figures. Opacity of each average  
369 spectra line has been lowered to allow general trends to be identified.

370

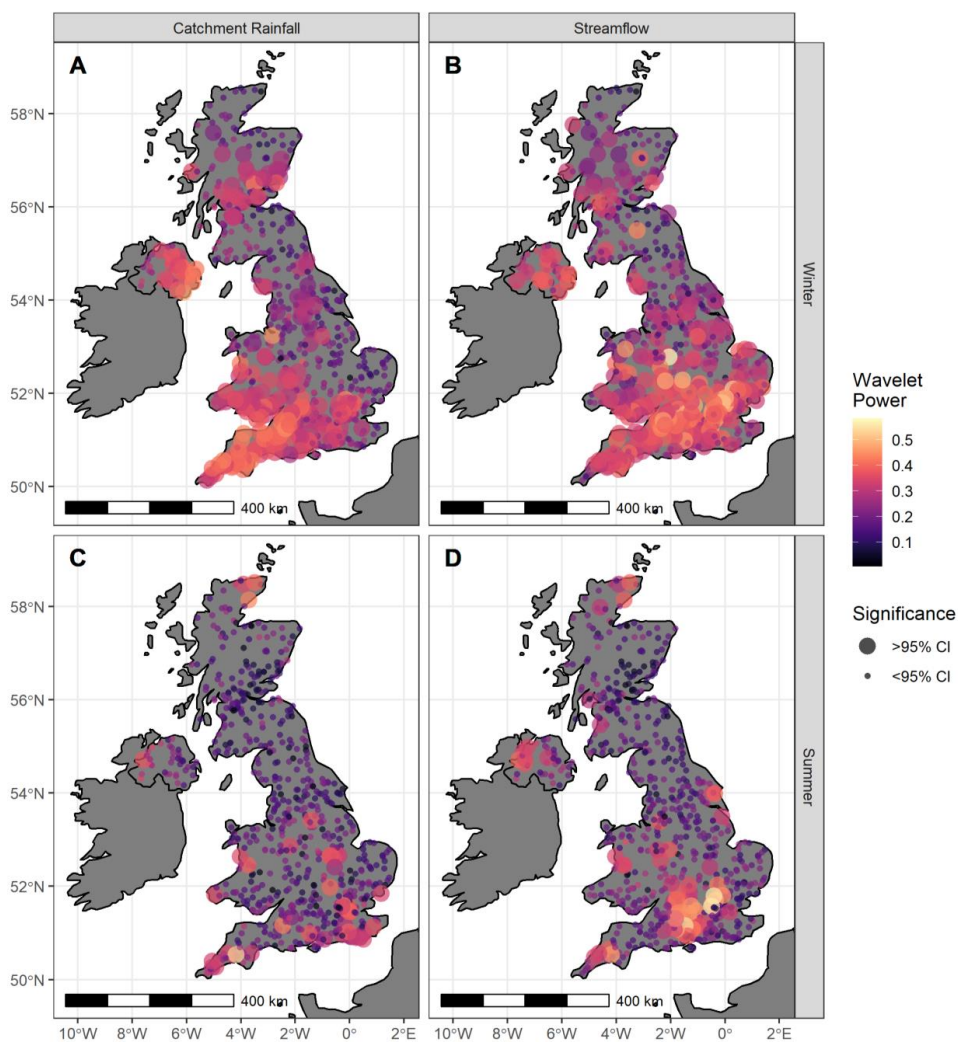




371

372 Figure 4 – As Fig. 3 but for catchment rainfall data.

373



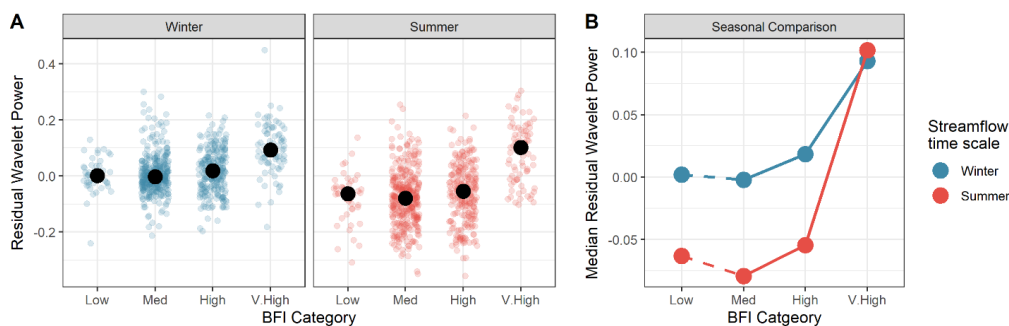
374

375 Figure 5 – Spatial distribution of ~7-year periodicity wavelet power and significance in  
376 catchment rainfall and streamflow, for winter and summer-averaged datasets.

377

378

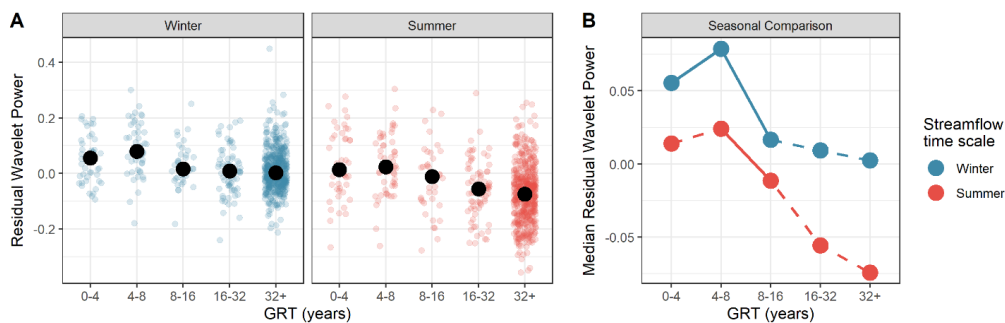
379



380

381 Figure 6 – A) shows jittered scatter plots for residual wavelet powers in winter and  
382 summer, categorised by BFI; bold black points mark the average residual wavelet power for each BFI  
383 category. B) compares these median residual wavelet powers with significant changes  
384 between groups shown as solid lines, and non-significant changes between groups shown in  
385 dashed lines.

386



387

388 Figure 7 – as figure 6 but for the Groundwater Response Times (GRT)

389

390

391

392

393

394

395

396

397

398

399

400



401 4. Discussion

402 4.1. Detecting a teleconnection between the NAO and UK Streamflow

403 Our results indicate that the dominant multi-annual periodicity in UK streamflow (and  
404 catchment rainfall) is that of an approximately 7-year cycle. This cycle closely compares to the  
405 principle 7-year periodicity documented in the strength of the NAO's atmospheric dipole, which  
406 has been associated with multi-annual periodicities in hydrometeorological records globally  
407 (Rust et al 2019; Meinke et al., 2005; Tremblay et al., 2011; Kuss and Gurdak, 2014; Holman  
408 et al., 2011; Neves et al., 2019). We show here that this ~7 year cycle is wide-spread within  
409 rainfall and streamflow variability across the UK, with the majority of streamflow and rainfall  
410 records assessed here exhibiting a coherent band of increased periodicity strength and  
411 significance around this 7-year frequency range. This, combined with greater significance for  
412 this periodicity, indicates an external control on this multi-annual mode of variability. As such,  
413 we build upon evidence in existing research that documents the teleconnection between the  
414 NAO and rainfall in Europe and show new evidence of the propagation of the NAO's ~7 year  
415 cycle to UK streamflow variability. Additionally, we detect expected differences between signal  
416 presence in summer and winter rainfall, showing the majority of NAO-like signals are present  
417 during the winter months, and absent in the summer. This generally agrees with existing  
418 research showing that NAO's control over European rainfall is primarily expressed in winter  
419 months (Trigo et al., 2004; West et al., 2019).

420 Olsen et al (2012) show that the NAO also exhibits a shorter (and weaker) 2-3 year periodicity  
421 between winter and summer NAO index values, and a ~6 year periodicity in summer index  
422 data. There are several other periodicities apparent in both our streamflow (Fig. 3) and rainfall  
423 (Fig. 4) wavelet power and significance, with peaks at ~2 years and ~5 years in the summer  
424 data. Therefore, it is possible that our results show that UK streamflow is driven by multiple  
425 periodicities in the NAO. Finally, our results (Figs. 3 and 4) indicate a 16-32 year periodicity in  
426 all the wavelet p-values which has previously been associated with the East Atlantic Pattern  
427 (EA) (Holman et al., 2011; Rust et al., 2019). As a secondary control on winter rainfall (after



428 the NAO) (Wallace and Gutzler, 1981), this would explain the weaker strength of the 16-32  
429 year cycle compared the NAO-like ~7 year cycle shown in the results. For the remainder of  
430 the paper, we will focus on the propagation on the NAO's principal periodicity (~7 years) that  
431 we have detected in both monthly and seasonal datasets.

432

#### 433 4.2. Controls on NAO-like signals in catchment rainfall

434 We provide new evidence that the influence of the NAO's ~7 year periodicity on UK rainfall is  
435 seen in the winter months, and is heavily localised to the Southwest of England, South Wales,  
436 the east coast of Northern Ireland and central band Scotland (Fig. 5). This is contrary to  
437 previous research that has typically found strongest relationships between the NAO Index and  
438 UK rainfall along the west coast of the UK, particularly the west coast of Scotland (Murphy and  
439 Washington, 2001; Fowler and Kilsby, 2002; West et al., 2019). Rust et al (2018) suggests  
440 that the NAO's control on UK rainfall variability may operate through two teleconnection  
441 pathways; atmospheric and oceanic, both with different temporal sensitivities. For instance, a  
442 positive (negative) NAO is known to drive increased (decreased) strength in the westerly storm  
443 tracks at an instantaneous timescale (Dawson et al., 2002; Walter and Graf, 2005), which  
444 subsequently drives wetter conditions on the west coast of the UK during the winter months  
445 (Walter and Graf, 2005). As such, we may expect methodologies that assess the  
446 instantaneous relationship between the NAO and rainfall (such as existing research) to show  
447 sensitivity to this atmospheric teleconnection route (e.g. Westerly Storm tracks). Conversely,  
448 the NAO is also known to increase the strength and meridional tilt of the Gulf Stream (Taylor  
449 and Stephens, 1998; Gangopadhyay et al., 2016; Watelet et al., 2017) which, as an oceanic  
450 process, filters out finer-scale variability and is sensitive to control at multi-annual timescales  
451 (Hurrell and Deser, 2010). It follows, therefore, that the Gulf Stream may be more sensitive to  
452 the NAO's long-term influence (such as its principal ~7 year periodicity) and relatively  
453 insensitive to its finer-scale variability (Rust et al 2018). Haarsma et al (2015) have shown  
454 that the Gulf Stream is particularly influential on rainfall variability in the South East of England



455 through its modulation of sea surface temperatures. As such, the increased strength in NAO-  
456 like signals in winter rainfall shown here in the South East of England may be an expression  
457 of the NAO's long-term control on the Gulf Stream.

458

#### 459 4.3. Hydrological drivers for signal strengths

460 We have shown that NAO-like periodicities are localised to specific regions in the UK in winter  
461 rainfall (Fig. 5a) and are negligible in summer rainfall (Fig. 5c). This suggests that NAO-like  
462 periodicities in summer streamflow do not originate from summer rainfall, and that catchment  
463 processes that drive winter rainfall signal propagation to summer streamflow (e.g. subsurface  
464 pathways (Haslinger *et al.*, 2014; Folland *et al.*, 2015; Barker *et al.*, 2016)) may inform our  
465 understanding of catchment controls on the NAO teleconnection with streamflow. Here, we  
466 provide statistically significant evidence that periodic NAO-like signals in rainfall are  
467 propagated to streamflow differently between winter and summer months, depending on the  
468 contribution from different hydrological pathways (and their response times). Furthermore, we  
469 provide evidence that pathways of specific response times propagate NAO-like periodic  
470 signals to UK streamflow more effectively than others, highlighting the catchment properties  
471 that may produce a sensitivity to the NAO teleconnection with streamflow. Below, we discuss  
472 how these relationships align with current hydrological understanding.

473 Rust *et al.* (2019) establishes that multi-annual NAO-like periodicities in groundwater level  
474 records are considerably stronger than those in co-located rainfall records. Groundwater  
475 behaviour generally exhibits longer autocorrelations than rainfall with negligible fine-scale  
476 variability (noise), due to the damping effect of subsurface hydrological pathways (Townley,  
477 1995; Dickinson, 2004; Gnann *et al.*, 2019). As such, groundwater can express a greater  
478 signal-to-noise ratio for low frequency variations (such as those produced by the NAO  
479 teleconnection) (Holman *et al.*, 2009; Rust *et al.*, 2018). By comparison, rainfall (which  
480 generally contains more fine-scale (hourly – daily) variability), exhibits a lower signal-to-noise



481 ratio which suppresses the proportional strength of multi-annual NAO-like signals (Meinke *et*  
482 *al.*, 2005; Brown, 2018). A parallel can be drawn here with hydrological pathway influence on  
483 streamflow, as surface pathways more closely reflect rainfall variability and subsurface  
484 pathways more closely reflect groundwater variability (Ockenden and Chappell, 2011;  
485 Kamruzzaman *et al.*, 2014; Mathias *et al.*, 2016; Gnann *et al.*, 2019).

486 Streamflow driven primarily by surface processes (e.g. BFI < 0.5) exhibits close-to-zero  
487 median RWP in winter (Fig. 6b), indicating surface pathways affect minimal modulation of  
488 NAO periodicity strength from winter rainfall to winter streamflow; likely due to their relatively  
489 short response times (minutes to days) (Mathias *et al.*, 2016). This also explains why the  
490 spatial footprint of NAO-like periodicities in winter streamflow (Fig. 5b) generally matches that  
491 of winter rainfall (Fig. 5a) as a greater proportion of surface pathway are active in response to  
492 greater in-season rainfall (due to more infiltration- or saturation-excess runoff from the land  
493 surface) (Ledingham *et al.*, 2019). Summer streamflow, where driven by surface pathways,  
494 exhibits a damping of NAO periodicities from winter rainfall (negative median RWPs), and no  
495 clear spatial structure of NAO-like periodicities. This is to be expected, given relative weakness  
496 of the NAO teleconnection with UK summer rainfall (as noted by Alexander *et al.*, (2005);  
497 Hurrell and Deser, (2010); West *et al.*, (2019), and indicated here) and the relative paucity of  
498 subsurface pathway contributions which can protract winter rainfall signals into summer  
499 months (Barker *et al.*, 2016). As a result, there are limited mechanisms to convey winter NAO  
500 periodicities to summer streamflow. Conversely, streamflow that is dominated by subsurface  
501 pathway influence (e.g. BFI > 0.75) exhibits the greatest NAO periodicities (Fig. 6b). We also  
502 see significant increases in NAO periodicity strength with increasing BFI in all but between the  
503 lowest two BFI categories (Low – Med). We therefore confirm our expectation that NAO  
504 periodicities in groundwater are propagated to streamflow via subsurface pathways. This  
505 relationship is also seen in the spatial footprints of NAO periodicities in winter (Fig. 5b) and  
506 summer streamflow (Fig. 5d). Gauges with the strongest NAO-like periods in summer and  
507 winter streamflow are found in catchments that are within, or that drain, the Chalk outcrop in





508 south central England. These catchments are known to be heavily driven by groundwater  
509 behaviour (Marsh and Hannaford, 2008). In Fig. 5b we see the spatial footprint of NAO  
510 periodicities in summer streamflow is localised to these Chalk-dominated catchments.  
511 Permeable catchments such as those on the Chalk aquifer are known to slowly respond to  
512 winter rainfall at a seasonal timescale (Hellwig and Stahl, 2018). As such, these catchments  
513 have sufficient subsurface pathway contribution to protract NAO periodicities in winter rainfall  
514 through to summer streamflow. Conversely, Fig. 5 also show some areas of the Chalk with  
515 relatively low NAO-like periods, such as the southern coast of England. Similarities can be  
516 seen here with Marchant and Bloomfield (2018) who identify discrete regions of groundwater  
517 level behaviour within the chalk aquifer, with varying autocorrelations. The Chalk of the south  
518 coast of England tend to have thinner superficial deposits and negligible glacial deposits  
519 (unlike those in the area of the Chalk outcrop), producing a faster recharge response to rainfall  
520 with shorter autocorrelations (Marsh and Hannaford, 2008; Marchant and Bloomfield, 2018).  
521 Dickinson *et al.*, (2014) highlights the importance of unsaturated zone thickness in modulating  
522 periodic signal progression, which may explain why catchments in the southern Chalk exhibit  
523 lower signal-to-noise ratios for NAO periodicities.

524 While the relationship between NAO periodicities and streamflow BFI indicates the importance  
525 of subsurface pathway contribution to teleconnection strength, properties of the subsurface  
526 pathways themselves are expected to modulate periodic signal propagation from rainfall to  
527 streamflow (Rust *et al.*, 2018). We show streamflow in catchments with shorter Groundwater  
528 Response Times (GRT) exhibit stronger NAO-like periodicities, but the strongest NAO  
529 periodicity is found in catchments with GRTs between 4 and 8 years. Townley (1995) shows  
530 that where the groundwater response time of a subsurface store is longer than a periodicity in  
531 recharge, the system will exhibit larger periodic variations in groundwater head but greater  
532 attenuation of periodic discharges at a streamflow boundary. This is because the pathway  
533 cannot equilibrate the periodic recharge to its hydraulic boundaries at a sufficient rate.  
534 Conversely, where the pathway response time is shorter than that of a periodicity in recharge,





535 groundwater discharge will show greater periodic variations as the entire pathway is able to  
536 convey this signal. This may explain the reduction in NAO periodicities seen as GRT increases  
537 in Fig. 6b. Where subsurface pathway response times are longer than the principal ~7 year  
538 periodicity of the NAO, we may expect the pathway to dampen the signal propagation to  
539 baseflow (Townley, 1995; Dickinson, 2004). However, this process fails to explain the reduced  
540 NAO periodicity strength seen in our results where GRT is less than the ~7 year NAO  
541 periodicity (seen principally in the winter streamflow data). As suggested by Najafi *et al.*,  
542 (2017) and Wilby, (2006), faster pathways can exhibit a weaker signal-to-noise ratio, when  
543 compared to slower pathways which are known to smooth signal propagation (Barker *et al.*,  
544 2016). As such, streamflow in catchments with the shortest GRT (i.e. 0-4 years) may exhibit  
545 greater response to finer scale variability in rainfall which supresses the relative strength of  
546 the NAO periodicity. This would also explain why summer streamflow does not show a  
547 similarly reduced NAO-like period strength for the 0-4 years GRT band, as summer streamflow  
548 generally would be expected to exhibit greater signal-to-noise ratios due to a greater  
549 proportion of slow pathway contribution. As such, our results suggest that, in addition to the  
550 described periodic signal modulations in Townley et al (1995), there is an ideal range of  
551 subsurface pathway response times that are long enough to produce a greater signal-to-noise  
552 ratio, but sufficiently short that there is minimal damping.

553

554 These results may have important implications for streamflow management, as we show that  
555 readily available estimates of BFI and GRT may be used to screen or identify catchments  
556 where teleconnection-driven multi-annual variability may be used to better inform risk  
557 estimation for hydrological extremes. This is particularly important for summer streamflow  
558 where streamflow services are often vulnerable to drought conditions (Visser *et al.*, 2019).

559

560



561 4. Conclusions

562 This paper assesses the degree to which the principal multi-annual periodicity (~7 years) of  
563 the NAO is present in streamflow and catchment rainfall records using the Continuous wavelet  
564 transform to identify multi-annual periodicities. We provide new evidence for the role of  
565 oceanic and atmospheric pathways in propagating NAO periodicities to catchment rainfall, by  
566 identifying spatial patterns of statistically significant NAO-like periodicities in UK catchment  
567 rainfall and streamflow. This may help further explicate the varying spatial extent of the NAO  
568 influence over Europe and the North Atlantic Region. Furthermore, we identify specific  
569 streamflow catchment characteristics that are most responsive to the NAO periodicities in  
570 catchment rainfall. We find that streamflow that is driven predominantly by subsurface pathway  
571 contributions often exhibit greater NAO-like periodicities, and that subsurface pathways with  
572 response times comparable in length to the ~7 year periodicity of the NAO produce the  
573 greatest sensitivity to the NAO teleconnection. These findings build on the fundamental  
574 understanding of periodic signal propagation through hydrological pathways and can be  
575 applied to streamflow catchments globally to identify areas of greater climatic teleconnection  
576 sensitivity. The ability to screen catchments for their potential teleconnection-driven multi-  
577 annual variability may have direct implications for water management decision making. For  
578 example, the permitting of surface water abstractions and their implications for ecologically  
579 sensitive streamflow systems. Such information may help to protect vulnerable habitats or aid  
580 appropriate investment in surface water abstraction infrastructure. Our results here make  
581 crucial steps towards a greater understanding of how climatic teleconnections can be used to  
582 improve water resource management practices.

583

584

585

586



587 **Data availability.**

588 The streamflow and precipitation data as well as the metadata used in this study are freely  
589 available at the NRFA website (<http://nrfa.ceh.ac.uk/>).

590

591 **Author contributions.**

592 WR designed the methodology and carried them out with supervision from all co-authors. WR  
593 prepared the article with contributions from all co-authors.

594

595 **Competing interests.**

596 The authors declare that they have no conflict of interest.

597

598 **Acknowledgements.**

599 This work was supported by the Natural Environment Research Council (grant numbers  
600 NE/M009009/1 and NE/L010070/1) and the British Geological Survey (Natural Environment  
601 Research Council). JB publishes with the permission of the Executive Director, British  
602 Geological Survey (NERC). MOC gratefully acknowledges funding for an Independent  
603 Research Fellowship from the UK Natural Environment Research Council (NE/P017819/1).  
604 We thank Angi Rosch and Harald Schmidbauer for making their wavelet package  
605 “WaveletComp” freely available.

606

607 **Financial support.**



608 This research has been supported by the Natural Environment Research Council (grant nos.  
609 NE/M009009/1 and NE/L010070/1), and MOC has been supported by an Independent  
610 Research Fellowship from the UK Natural Environment Research Council (NE/P017819/1).

611

## 612 **References**

613 A Lane, R., Coxon, G., E Freer, J., Wagener, T., J Johnes, P., P Bloomfield, J., Greene, S.,  
614 J A Macleod, C. and M Reaney, S.: Benchmarking the predictive capability of hydrological  
615 models for river flow and flood peak predictions across over 1000 catchments in Great  
616 Britain, *Hydrology and Earth System Sciences*, 23, 4011–4032. [https://doi.org/10.5194/hess-](https://doi.org/10.5194/hess-23-4011-2019)  
617 23-4011-2019, 2019.

618 Acreman, M. C. and Dunbar, M. J.: Defining environmental river flow requirements – a  
619 review, *Hydrology and Earth System Sciences*, 8, 861–876. [https://doi.org/10.5194/hess-8-](https://doi.org/10.5194/hess-8-861-2004)  
620 861-2004, 2004.

621 Alexander, L. V., Tett, S. F. B. and Jonsson, T.: Recent observed changes in severe storms  
622 over the United Kingdom and Iceland, *Geophysical Research Letters*, 32, 1–4.  
623 <https://doi.org/10.1029/2005GL022371>, 2005.

624 Barker, L. J., Hannaford, J., Chiveron, A. and Svensson, C.: From meteorological to  
625 hydrological drought using standardised indicators, *Hydrology and Earth System Sciences*,  
626 20, 2483–2505. <https://doi.org/10.5194/hess-20-2483-2016>, 2016.

627 Bloomfield, J. P., Allen, D. J. and Griffiths, K. J.: Examining geological controls on baseflow  
628 index (BFI) using regression analysis: An illustration from the Thames Basin, UK, *Journal of*  
629 *Hydrology*. Elsevier B.V., 373, 164–176. <https://doi.org/10.1016/j.jhydrol.2009.04.025>, 2009.

630 Bouwer, L. M., Vermaat, J. E. and Aerts, J. C. J. H.: Winter atmospheric circulation and river  
631 discharge in northwest Europe, *Geophysical Research Letters*, 33, L06403.  
632 <https://doi.org/10.1029/2005GL025548>, 2006.



- 633 Bracken, L. J., Wainwright, J., Ali, G. A., Tetzlaff, D., Smith, M. W., Reaney, S. M. and Roy,  
634 A. G.: Concepts of hydrological connectivity: Research approaches, Pathways and future  
635 agendas, *Earth-Science Reviews*. Elsevier B.V., 119, 17–34.  
636 <https://doi.org/10.1016/j.earscirev.2013.02.001>, 2013.
- 637 Brown, S. J.: The drivers of variability in UK extreme rainfall, *International Journal of*  
638 *Climatology*, 38, e119–e130. <https://doi.org/10.1002/joc.5356>, 2018.
- 639 Burt, T. P. and Howden, N. J. K.: North Atlantic Oscillation amplifies orographic precipitation  
640 and river flow in upland Britain, *Water Resources Research*, 49.  
641 <https://doi.org/10.1002/wrcr.20297>, 2013.
- 642 Carr, E. J. and Simpson, M. J.: Accurate and efficient calculation of response times for  
643 groundwater flow, *Journal of Hydrology*. Elsevier B.V., 558, 470–481.  
644 <https://doi.org/10.1016/j.jhydrol.2017.12.023>, 2018.
- 645 Chaudhuri, A. H., Gangopadhyay, A. and Bisagni, J. J.: Response of the Gulf Stream  
646 transport to characteristic high and low phases of the North Atlantic Oscillation, *Ocean*  
647 *Modelling*, 39, 220–232. <https://doi.org/10.1016/j.ocemod.2011.04.005>, 2011.
- 648 Chiverton, A., Hannaford, J., Holman, I. P., Corstanje, R., Prudhomme, C., Hess, T. M. and  
649 Bloomfield, J. P.: Using variograms to detect and attribute hydrological change, *Hydrology*  
650 *and Earth System Sciences*, 19, 2395–2408. <https://doi.org/10.5194/hess-19-2395-2015>,  
651 2015.
- 652 Chun, K. P., Wheeler, H. S. and Onof, C. J.: Streamflow estimation for six UK catchments  
653 under future climate scenarios, *Hydrology Research*, 40, 96–112.  
654 <https://doi.org/10.2166/nh.2009.086>, 2009.
- 655 Crossman, J., Futter, M. N., Whitehead, P. G., Stainsby, E., Baulch, H. M., Jin, L., Oni, S. K.,  
656 Wilby, R. L. and Dillon, P. J.: Flow pathways and nutrient transport mechanisms drive  
657 hydrochemical sensitivity to climate change across catchments with different geology and



- 658 topography, *Hydrology and Earth System Sciences*, 18, 5125–5148.  
659 <https://doi.org/10.5194/hess-18-5125-2014>, 2014.
- 660 Cuthbert, M. O., Gleeson, T., Moosdorf, N., Befus, K. M., Schneider, A., Hartmann, J. and  
661 Lehner, B.: Global patterns and dynamics of climate–groundwater interactions, *Nature*  
662 *Climate Change*. Nature Publishing Group, 9, 137–141. [https://doi.org/10.1038/s41558-018-](https://doi.org/10.1038/s41558-018-0386-4)  
663 0386-4, 2019.
- 664 Dawson, A., Elliott, L., Noone, S., Hickey, K., Holt, T., Wadhams, P. and Foster, I.: Historical  
665 storminess and climate ‘see-saws’ in the North Atlantic region, *Marine Geology*, 210, 247–  
666 259. <https://doi.org/10.1016/j.margeo.2004.05.011>, 2004.
- 667 Dawson, A. G., Hickey, K., Holt, T., Elliott, L., Dawson, S., Foster, I. D. L., Wadhams, P.,  
668 Jonsdottir, I., Wilkinson, J., McKenna, J., Davis, N. R. and Smith, D. E.: Complex North  
669 Atlantic Oscillation (NAO) Index signal of historic North Atlantic storm-track changes, *The*  
670 *Holocene*, 12, 363–369. <https://doi.org/10.1191/0959683602hl552rr>, 2002.
- 671 Dickinson, J. E.: Inferring time-varying recharge from inverse analysis of long-term water  
672 levels, *Water Resources Research*, 40, 1–15. <https://doi.org/10.1029/2003WR002650>, 2004.
- 673 Dickinson, J. E., Ferré, T. P. A., Bakker, M. and Crompton, B.: A Screening Tool for  
674 Delineating Subregions of Steady Recharge within Groundwater Models, *Vadose Zone*  
675 *Journal*, 13, 1–15. <https://doi.org/10.2136/vzj2013.10.0184>, 2014.
- 676 Faust, J. C., Fabian, K., Milzer, G., Giraudeau, J. and Knies, J.: Norwegian fjord sediments  
677 reveal NAO related winter temperature and precipitation changes of the past 2800 years,  
678 *Earth and Planetary Science Letters*, 435, 84–93. <https://doi.org/10.1016/j.epsl.2015.12.003>,  
679 2016.
- 680 Folland, C. K., Hannaford, J., Bloomfield, J. P., Kendon, M., Svensson, C., Marchant, B. P.,  
681 Prior, J. and Wallace, E.: Multi-annual droughts in the English Lowlands: a review of their  
682 characteristics and climate drivers in the winter half-year, *Hydrology and Earth System*



- 683 Sciences, 19, 2353–2375. <https://doi.org/10.5194/hess-19-2353-2015>, 2015.
- 684 Fowler, H. J. and Kilsby, C. G.: Precipitation and the North Atlantic Oscillation: a study of  
685 climatic variability in northern England, *International Journal of Climatology*, 22, 843–866.  
686 <https://doi.org/10.1002/joc.765>, 2002.
- 687 Frankignoul, C., de Coëtlogon, G., Joyce, T. M. and Dong, S.: Gulf Stream Variability and  
688 Ocean–Atmosphere Interactions, *Journal of Physical Oceanography*, 31, 3516–3529.  
689 [https://doi.org/10.1175/1520-0485\(2002\)031<3516:GSVAOA>2.0.CO;2](https://doi.org/10.1175/1520-0485(2002)031<3516:GSVAOA>2.0.CO;2), 2001.
- 690 Fritier, N., Massei, N., Laignel, B., Durand, A., Dieppois, B. and Deloffre, J.: Links between  
691 NAO fluctuations and inter-annual variability of winter-months precipitation in the Seine River  
692 watershed (north-western France), *Comptes Rendus - Geoscience. Academie des sciences*,  
693 344, 396–405. <https://doi.org/10.1016/j.crte.2012.07.004>, 2012.
- 694 Gangopadhyay, A., Chaudhuri, A. H. and Taylor, A. H.: On the nature of temporal variability  
695 of the gulf stream path from 75° to 55°W, *Earth Interactions*, 20. [https://doi.org/10.1175/EI-D-](https://doi.org/10.1175/EI-D-15-0025.1)  
696 15-0025.1, 2016.
- 697 Gericke, O. J. and Smithers, J. C.: Revue des méthodes d'évaluation du temps de réponse  
698 d'un bassin versant pour l'estimation du débit de pointe, *Hydrological Sciences Journal*.  
699 Taylor & Francis, 59, 1935–1971. <https://doi.org/10.1080/02626667.2013.866712>, 2014.
- 700 Gnann, S. J., Howden, N. J. K. and Woods, R. A.: Hydrological signatures describing the  
701 translation of climate seasonality into streamflow seasonality, *Hydrology and Earth System*  
702 *Sciences Discussions*, 1–30. <https://doi.org/10.5194/hess-2019-463>, 2019.
- 703 Guillod, B. P., Jones, R. G., Dadson, S. J., Coxon, G., Bussi, G., Freer, J., Kay, A. L.,  
704 Massey, N. R., Sparrow, S. N., Wallom, D. C. H., Allen, M. R. and Hall, J. W.: A large set of  
705 potential past, present and future hydro-meteorological time series for the UK, *Hydrology*  
706 *and Earth System Sciences*, 22, 611–634. <https://doi.org/10.5194/hess-22-611-2018>, 2018.
- 707 Hannaford, J. and Harvey, C.: UK seasonal river flow variability in near-natural catchments,



708 regional outflows and long hydrometric records, BHS Third International Symposium,  
709 Managing Consequences of a Changing Global Environment, 1–7, 2010.

710 Haslinger, K., Koffler, D., Schöner, W. and Laaha, G.: Exploring the link between  
711 meteorological drought and streamflow: Effects of climate-catchment interaction, *Water*  
712 *Resources Research*, 50, 2468–2487. <https://doi.org/10.1002/2013WR015051>, 2014.

713 Heape, R., Hirschi, J. and Sinha, B.: Asymmetric response of European pressure and  
714 temperature anomalies to NAO positive and NAO negative winters, *Weather*, 68, 73–80.  
715 <https://doi.org/10.1002/wea.2068>, 2013.

716 Hellwig, J. and Stahl, K.: An assessment of trends and potential future changes in  
717 groundwater-baseflow drought based on catchment response times, *Hydrology and Earth*  
718 *System Sciences*, 22, 6209–6224. <https://doi.org/10.5194/hess-22-6209-2018>, 2018.

719 Holman, I. P., Rivas-Casado, M., Howden, N. J. K., Bloomfield, J. P. and Williams, A. T.:  
720 Linking North Atlantic ocean-atmosphere teleconnection patterns and hydrogeological  
721 responses in temperate groundwater systems, *Hydrological Processes*. John Wiley & Sons,  
722 Ltd, 23, 3123–3126. <https://doi.org/10.1002/hyp.7466>, 2009.

723 Holman, I., Rivas-Casado, M., Bloomfield, J. P. and Gurdak, J. J.: Identifying non-stationary  
724 groundwater level response to North Atlantic ocean-atmosphere teleconnection patterns  
725 using wavelet coherence, *Hydrogeology Journal*, 19, 1269–1278.  
726 <https://doi.org/10.1007/s10040-011-0755-9>, 2011.

727 Hurrell, J. W.: Decadal Trends in the North Atlantic Oscillation: Regional Temperature and  
728 Precipitation, 1995.

729 Hurrell, J. W. and Deser, C.: North Atlantic climate variability: The role of the North Atlantic  
730 Oscillation, *Journal of Marine Systems*, 79, 231–244.  
731 <https://doi.org/10.1016/j.jmarsys.2009.11.002>, 2010.

732 Hurrell, J. W., Kushnir, Y., Ottersen, G. and Visbeck, M.: An Overview of the North Atlantic





- 733 Oscillation, in *The North Atlantic Oscillation: Climatic Significance and Environmental*  
734 *Impact*. American Geophysical Union, 1–35. <https://doi.org/10.1029/134GM01>, 2003.
- 735 Jelena Luković, Branislav Bajat, Dragan Blagojević, M. K.: Spatial pattern of North Atlantic  
736 Oscillation impact on rainfall in Serbia, *Spatial Statistics*. Elsevier Ltd.  
737 <https://doi.org/10.1016/j.spasta.2015.04.007>, 2014.
- 738 Kamruzzaman, M., Shahriar, M. S. and Beecham, S.: Assessment of short term rainfall and  
739 stream flows in South Australia, *Water (Switzerland)*, 6, 3528–3544.  
740 <https://doi.org/10.3390/w6113528>, 2014.
- 741 Kingston, D. G., Lawler, D. M. and McGregor, G. R.: Linkages between atmospheric  
742 circulation, climate and streamflow in the northern North Atlantic: research prospects,  
743 *Progress in Physical Geography*, 30, 143–174. <https://doi.org/10.1191/0309133306pp471ra>,  
744 2006.
- 745 Kronholm, S. and Capel, P.: Estimation of time-variable fast flow path  
746 chemical concentrations for application in tracer-based hydrograph separation analyses,  
747 *Journal of the American Water Resources Association*, 52, 6881–6896.  
748 <https://doi.org/10.1002/2016WR018797>, 2016.
- 749 Kuss, A. M. and Gurdak, J. J.: Groundwater level response in U.S. principal aquifers to  
750 ENSO, NAO, PDO, and AMO, *JOURNAL OF HYDROLOGY*, 519, 1939–1952.  
751 <https://doi.org/10.1016/j.jhydrol.2014.09.069>, 2014.
- 752 Lawler, D., McGregor, G. and Phillips, I.: Influence of atmospheric circulation changes and  
753 regional climate variability on river flow and suspended sediment fluxes in southern Iceland,  
754 *Geophysical Research Letters*. Elsevier B.V., 17, 3195–3223. <https://doi.org/10.1002/hyp>,  
755 2011.
- 756 Ledingham, J., Archer, D., Lewis, E., Fowler, H. and Kilsby, C.: Contrasting seasonality of  
757 storm rainfall and flood runoff in the UK and some implications for rainfall-runoff methods of



- 758 flood estimation, *Hydrology Research*, 50, 1309–1323. <https://doi.org/10.2166/nh.2019.040>,  
759 2019.
- 760 López-Moreno, J. I., Vicente-Serrano, S. M., Morán-Tejeda, E., Lorenzo-Lacruz, J., Kenawy,  
761 a. and Beniston, M.: Effects of the North Atlantic Oscillation (NAO) on combined temperature  
762 and precipitation winter modes in the Mediterranean mountains: Observed relationships and  
763 projections for the 21st century, *Global and Planetary Change*. Elsevier B.V., 77, 62–76.  
764 <https://doi.org/10.1016/j.gloplacha.2011.03.003>, 2011.
- 765 Marchant, B. P. and Bloomfield, J. P.: Spatio-temporal modelling of the status of  
766 groundwater droughts, *Journal of Hydrology*. Elsevier, 564, 397–413.  
767 <https://doi.org/10.1016/J.JHYDROL.2018.07.009>, 2018.
- 768 Marsh, T. and Hannaford, J.: *UK Hydrometric Register. Hydrological data UK series*. Centre  
769 for Ecology and Hydrology, 2008.
- 770 Mathias, S. A., McIntyre, N. and Oughton, R. H.: A study of non-linearity in rainfall-runoff  
771 response using 120 UK catchments, *Journal of Hydrology*. Elsevier B.V., 540, 423–436.  
772 <https://doi.org/10.1016/j.jhydrol.2016.06.039>, 2016.
- 773 Meinke, H., deVoil, P., Hammer, G. L., Power, S., Allan, R., Stone, R. C., Folland, C. and  
774 Potgieter, A.: Rainfall variability of decadal and longer time scales: Signal or noise?, *Journal*  
775 *of Climate*, 18, 89–90. <https://doi.org/10.1175/JCLI-3263.1>, 2005.
- 776 Misumi, R., Bell, V. A. and Moore, R. J.: River flow forecasting using a rainfall disaggregation  
777 model incorporating small-scale topographic effects, *Meteorological Applications*, 8, 297–  
778 305. <https://doi.org/10.1017/S135048270100305X>, 2001.
- 779 Murphy, S. J. and Washington, R.: United Kingdom and Ireland precipitation variability and  
780 the North Atlantic sea-level pressure field, *International Journal of Climatology*, 21, 939–959.  
781 <https://doi.org/10.1002/joc.670>, 2001.
- 782 Najafi, M. R., Zwiers, F. W. and Gillett, N. P.: Attribution of Observed Streamflow Changes in



- 783 Key British Columbia Drainage Basins, *Geophysical Research Letters*, 44, 11,012-11,020.  
784 <https://doi.org/10.1002/2017GL075016>, 2017.
- 785 Nathan, R. J. and McMahon, T. A.: Evaluation of automated techniques for base flow and  
786 recession analyses, *Water Resources Research*, 26, 1465–1473.  
787 <https://doi.org/10.1029/WR026i007p01465>, 1990.
- 788 Neves, M. C., Jerez, S. and Trigo, R. M.: The response of piezometric levels in Portugal to  
789 NAO, EA, and SCAND climate patterns, *Journal of Hydrology. Elsevier*, 568, 1105–1117.  
790 <https://doi.org/10.1016/J.JHYDROL.2018.11.054>, 2019.
- 791 Ockenden, M. C. and Chappell, N. A.: Identification of the dominant runoff pathways from  
792 data-based mechanistic modelling of nested catchments in temperate UK, *Journal of*  
793 *Hydrology. Elsevier B.V.*, 402, 71–79. <https://doi.org/10.1016/j.jhydrol.2011.03.001>, 2011.
- 794 Riaz, S. M. F., Iqbal, M. J. and Hameed, S.: Impact of the North Atlantic Oscillation on winter  
795 climate of Germany, *Tellus, Series A: Dynamic Meteorology and Oceanography. Taylor &*  
796 *Francis*, 69, 1–10. <https://doi.org/10.1080/16000870.2017.1406263>, 2017.
- 797 Rousseau-Gueutin, P., Love, A. J., Vasseur, G., Robinson, N. I., Simmons, C. T. and De  
798 Marsily, G.: Time to reach near-steady state in large aquifers, *Water Resources Research*,  
799 49, 6893–6908. <https://doi.org/10.1002/wrcr.20534>, 2013.
- 800 Rust, W., Holman, I., Bloomfield, J., Cuthbert, M. and Corstanje, R.: Understanding the  
801 potential of climate teleconnections to project future groundwater drought, *Hydrology and*  
802 *Earth System Sciences*, 23, 3233–3245. <https://doi.org/10.5194/hess-23-3233-2019>, 2019.
- 803 Rust, W., Holman, I., Corstanje, R., Bloomfield, J. and Cuthbert, M.: A conceptual model for  
804 climatic teleconnection signal control on groundwater variability in Europe, *Earth-Science*  
805 *Reviews*, 177, 164–174. <https://doi.org/10.1016/j.earscirev.2017.09.017>, 2018.
- 806 Su, L., Miao, C., Borthwick, A. G. L. and Duan, Q.: Wavelet-based variability of Yellow River  
807 discharge at 500-, 100-, and 50-year timescales, *Gondwana Research*, 49, 94–105.



- 808 <https://doi.org/10.1016/j.gr.2017.05.013>, 2017.
- 809 Tabari, H., Hosseinzadeh Talaei, P., Shifteh Some'e, B. and Willems, P.: Possible  
810 influences of North Atlantic Oscillation on winter reference evapotranspiration in Iran, *Global*  
811 *and Planetary Change*. Elsevier B.V., 117, 28–39.  
812 <https://doi.org/10.1016/j.gloplacha.2014.03.006>, 2014.
- 813 Taylor, A. H. and Stephens, J. A.: The North Atlantic Oscillation and the latitude of the Gulf  
814 Stream, *Tellus, Series A: Dynamic Meteorology and Oceanography*, 50, 134–142.  
815 <https://doi.org/10.3402/tellusa.v50i1.14517>, 1998.
- 816 Townley, L. R.: The response of aquifers to periodic forcing, *Advances in Water Resources*,  
817 18, 125–146. [https://doi.org/10.1016/0309-1708\(95\)00008-7](https://doi.org/10.1016/0309-1708(95)00008-7), 1995.
- 818 Trigo, R. M., Osborn, T. J. and Corte-real, J. M.: The North Atlantic Oscillation influence on  
819 Europe: climate impacts and associated physical mechanisms, *Climate Research*, 20, 9–17.  
820 <https://doi.org/10.3354/cr020009>, 2002.
- 821 Trigo, R. M., Pozo-Vazquez, D., Osborn, T. J., Castro-Diez, Y., Gamiz-Fortis, S. and  
822 Esteban-Parra, M. J.: North Atlantic oscillation influence on precipitation, river flow and water  
823 resources in the Iberian peninsula, *International Journal of Climatology*, 24, 925–944.  
824 <https://doi.org/10.1002/joc.1048>, 2004.
- 825 Uvo, C. B.: Analysis and regionalization of northern European winter precipitation based on  
826 its relationship with the North Atlantic oscillation, *International Journal of Climatology*, 23,  
827 1185–1194. <https://doi.org/10.1002/joc.930>, 2003.
- 828 Visser, A., Beevers, L. and Patidar, S.: The impact of climate change on hydroecological  
829 response in chalk streams, *Water (Switzerland)*, 11. <https://doi.org/10.3390/w11030596>,  
830 2019.
- 831 Wallace, J. M. and Gutzler, D. S.: Teleconnections in the Geopotential Height Field during  
832 the Northern Hemisphere Winter, *Monthly Weather Review*, 784–812.



- 833 [https://doi.org/10.1175/1520-0493\(1981\)109<0784:TITGHF>2.0.CO;2](https://doi.org/10.1175/1520-0493(1981)109<0784:TITGHF>2.0.CO;2), 1981.
- 834 Walter, K. and Graf, H.-F.: The North Atlantic variability structure, storm tracks, and  
835 precipitation depending on the polar vortex strength, *Atmospheric Chemistry and Physics*, 4,  
836 6127–6148. <https://doi.org/1680-7324/acp/2005-5-239>, 2005.
- 837 Watelet, S., Beckers, J. M. and Barth, A.: Reconstruction of the Gulf Stream from 1940 to  
838 the present and correlation with the North Atlantic Oscillation, *Journal of Physical*  
839 *Oceanography*, 47, 2741–2754. <https://doi.org/10.1175/JPO-D-17-0064.1>, 2017.
- 840 West, H., Quinn, N. and Horswell, M.: Regional rainfall response to the North Atlantic  
841 Oscillation (NAO) across Great Britain, *Hydrology Research*, 50, 1549–1563.  
842 <https://doi.org/10.2166/nh.2019.015>, 2019.
- 843 Wilby, R. L.: When and where might climate change be detectable in UK river flows?,  
844 *Geophysical Research Letters*, 33, 1–5. <https://doi.org/10.1029/2006GL027552>, 2006.
- 845 Wrzesiński, D. and Paluszkiwicz, R.: Spatial differences in the impact of the North Atlantic  
846 Oscillation on the flow of rivers in Europe, *Hydrology Research*, 42, 30–39.  
847 <https://doi.org/10.2166/nh.2010.077>, 2011.
- 848 Zhang, X. J., Jin, L. Y., Chen, C. Z., Guan, D. S. and Li, M. Z.: Interannual and interdecadal  
849 variations in the North Atlantic Oscillation spatial shift, *Chinese Science Bulletin*, 56, 2621–  
850 2627. <https://doi.org/10.1007/s11434-011-4607-8>, 2011.
- 851